# Gel-type ion exchange resin stabilized Pd-Bi nanoparticles for the glycerol oxidation in liquid phase

Stanislav Vajíček [1], Magdaléna Štolcová [1*], Alexander Kaszonyi [1], Matej Mičušík [2], Pavol Alexy [3], Patrizia Canton [4], György Onyestyák [5], Szabolcs Harnos [5], Ferenc Lónyi [5], József Valyon [5]

[1] *Department of Organic Technology, Joint Slovak-Hungarian Laboratory for Development of Catalyzed Chemical Processes of Biomass Utilization, Slovak University of Technology, Radlinského 9, 81237 Bratislava, Slovak Republic*
[2] *Polymer Institute, Slovak Academy of Sciences, Dúbravská cesta 9, 845 41 Bratislava, Slovak Republic*
[3] *Department of Plastics and Rubber, Slovak University of Technology, Radlinského 9, 81237 Bratislava, Radlinského 9, Slovak Republic*
[4] *Dipartimento di Chimica Fisica, Università di Venezia, via Torino 155/b, 30170 Venezia-Mestre, Italy*
[5] *Institute of Materials and Research Centre for Natural Science, Joint Slovak-Hungarian Laboratory for Development of Catalyzed Chemical Processes of Biomass Utilization, Magyar tudósok körútja 2, H-1117 Budapest, Hungary*

[*] Corresponding author. Tel.: +421 259325373, E-mail address: magdalena.stolcova@stuba.sk (M. Štolcová)

## Abstract

Palladium – bismuth nanoparticles were supported into strongly basic anion-exchange resin of gel-type and tested as catalysts for the selective oxidation of glycerol with molecular oxygen at atmospheric pressure. Detailed study of the preparation of immobilized palladium(II)-bismuth(III) precursors into the resin and the reduction of such metallated complexes either by sodium borohydride or molecular hydrogen were undertaken. Based on the spectroscopic characterizations was found that the ion-exchange reaction tends to reach a fast saturation and the reduction method significantly influences the size of crystalline Pd particles, the electronic states and surface configuration of the Pd-Bi species. The size of palladium particles differs negligible by the variation of the metal loading in the range of 1 – 3 wt. %; however, the latter has a major impact on the reaction rate as well as the yield of the glyceric acid and tartronic acid. The catalyst 3%Pd-1%Bi where the bismuth was deposited on the palladium particles (3.4 nm) formed after borohydride reduction exhibited at 50°C and 200 mL $min^{-1}$ of oxygen flow-rate 95 % conversion of glycerol and higher than 63 % yield towards target acids after 3 hours of reaction. More than 90 % of glycerol initial conversion and the selectivity of target acids 73 % had been able to be reached after five consecutive catalytic cycles without extra catalyst treatment and reactivation. The interaction between active metal species and the support may influence the performance of catalyst.

**Keywords:** Gel-type anion-exchange resin, Pd–Bi nanoparticles, Glycerol liquid-phase oxidation, Glyceric acid, Tartronic acid

## 1. Introduction

Glycerol belongs to platform molecules derivable from biomass. It is readily available from the industrial bio-diesel production through transesterification of triglycerides with methanol, where 100 kg of glycerol, as by-product is formed per 1 tone of biodiesel (10 wt. % of the total biodiesel production). The recently developed biofuel manufacturing procedures from non-edible crops mostly cultivated on poor soil, algae lipids, animal or waste fats appear to be ethically acceptable towards the conversion of biomass to fuels and chemicals (as a second/third generation biofuels) [1]. In this respect, the valorization of glycerol is important because it may help to increase the carbon balance (atom efficiency) as well as to improve the economy of bio-diesel production [2].

Over the past few years many studies have been focused on the glycerol transformation by various catalytic processes including oxidation, hydrogenolysis, dehydration, etherification, esterification, acetalisation, carboxylation, a. o., to obtain alternative commodity and fine chemicals [3-8]. Among them, the catalytic oxidation of glycerol with molecular oxygen or air leading to the formation of several very highly value-added oxygenated compounds, such as dihydroxyacetone, glyceric, tartronic, glycolic and hydroxypyruvic acids has been attracted great attention [3,9]. The commercially available oxidation products are actually produced by using inorganic oxidizing agents (such as, permanganate, chromic salts or nitric acid) or by low productivity fermentation processes [10]. The selective oxidation of glycerol using heterogeneous catalysts could be an efficient alternative for the production of these high value-added chemicals by environmentally friendly methods. Among the various target compounds accessible by glycerol oxidation, glyceric acid could be an important intermediate for amino acids synthesis [3] or for further oxidation products such as tartronic acid and mesoxalic acid [11]. Tartronic acid found use as a pharmaceutical in the treatment of osteoporosis and obesity; moreover, due to its characteristic oxygen scavenger property it could be an anti-corrosive protecting agent and an oxygen absorber in food industry [3].

A variety of noble metal-based monometallic and bimetallic catalysts have been reported for liquid phase oxidation of glycerol. The metals used in these studies included Pd, Pt, Au, Pt-Bi, Au-Pd, Au-Pt supported usually on carbonaceous materials (active carbon, charcoal, graphite, carbon nanotubes) [12-23], but metal oxides ($TiO_2$, $CeO_2$, $Al_2O_3$, $Nb_2O_5$, $V_2O_5$, $Ta_2O_5$) [24-27], $MgAl_2O_4$-spinels [28] or hydrotalcite [29] have also been employed. A second metal or promoter is added sometimes in order to improve the activity and/or selectivity, to inhibit the over-oxidation or to prevent the deactivation. Bismuth is one of the well-established promoters of supported Pd and Pt catalysts for the selective liquid phase oxidation of alcohols [30-32]. The promoter itself is inactive for the oxidation reactions, but when associated with the noble metal, it can considerably suppress the oxygen poisoning of the Pd surface [30], increase the reaction rate [33,34] and modify the selectivity [12,13,35]. Models proposed to interpret the role of promoters include the formation of i) a complexes between an α-

functionalized alcohol, a surface Pt or Pd atom and a promoter [36], ii) a bifunctional catalysis [37], iii) an ordered alloy [34], iv) Bi may act as cocatalyst due to its higher affinity for oxygen and protect Pt or Pd from overoxidation [36] or v) as a homogeneous catalyst by leached promoter [31]. However, the most accepted role of Bi promotion is the geometric (blocking) effect of a fraction of active sites centered on the noble metal, since providing different coordination environment for substrate and in turn improving the catalytic performance of the original catalysts [12,38]. For this reason special techniques were developed to deposit Bi mainly as adatom onto the supported Pd particles [36,39,40].

It is generally accepted that the nature, the structure and the texture of the catalyst support can yield a beneficial improvement in the catalytic performance. Over the last years, polymeric materials having varied chemical structure of the backbone, cross-linking and functional groups, different morphology, porosity and macroscopic dimension [41-45] could efficiently immobilized the monometallic or the bimetallic nanoclusters, thus provide a solution to the problem with reusability without aggregation of nanoclusters and leaching of metals [46-48]. Despite the number of investigation in this field, there are almost missing data on the use of commercial ion exchange resin as a support for the catalytic oxidation of glycerol. Up to the present day, a commercial weak anion-exchange resin with a macroporous structure was employed for depositing Au (Dowex M-43) [49] or Pt (Mitsubishi WA-30) [50] nanoparticles as a catalyst for the liquid phase oxidation of glycerol to obtaining glyceric acid. In the work of Prati et al. [49] the metallic sol stabilized by tetrahydroxymethyl phosphonium chloride showed higher activity. Gross et al. [46] demonstrated the effect of competitor anion which is the ion used during the support pre-treatment. Very recently, Mimura et al. [51] reported nano-sized gold-palladium particles stabilized in the gel-type anion exchange resin (Amberlite IRA402BLCL) as catalyst for liquid phase oxidation of glycerol at 333 K and with the initial pressure of molecular oxygen 1.0 MPa and 0.5 MPa in a closed batch reactor and in a flow type reactor.

Currently, a wide range of polymeric functional resins based on polystyrene are being supplied to the market by the ion-exchange resin manufacturers for common [52] or specific applications [53,54]. Intermediate cross-linked densities lead to gel-type polymers that are swell-able in an appropriate solvent, but are non-porous in dry state. The swelling behavior of the polymer support facilitates the dispersion of the metal precursors in the polymeric framework, which together with functional groups assist in the immobilization of the metal particles [55]. The formation of swollen-gel phase is favorable for the involvement of all reactants in the catalytic reaction.

In the present contribution we have investigated the catalytic activity of Pd - Bi nanoparticles supported into a strongly basic anion-exchange resin of gel-type (Dowex®1x4) for oxidation of glycerol using molecular oxygen under basic conditions and at atmospheric pressure. The objective was focused on the preparation of immobilized palladium(II)-bismuth(III) precursors into the resin and the reduction of the metallated complexes of resin either by sodium borohydride or molecular hydrogen. In addition, the effect of the metals loading, the reaction temperature and the catalyst recycling was studied for oxidation of glycerol to obtain glyceric acid and tartronic acid.

## 2. Experimental

### *2.1. Materials*

$PdCl_2$ (40 wt. % solution in $HCl/H_2O$), $BiCl_3$ (> 98%) from Alfa Aesar, $NaBH_4$ (> 99%) from Sigma-Aldrich were used. Dowex®1x4 chloride form microgel resin (particle size 100-200 mesh, tetraalkylammonium groups) purchased from Fluka and glycerol (> 98%) from Palma Tumys. All other chemicals were analytical reagent grade.

### *2.2. Catalysts preparation*

The chloride form of Dowex®1x4 strong anion exchange resin prior to use was washed with 1 M KCl, deionized water and isopropanol; subsequently dried at 50°C and reduced pressure (10 kPa).

Precursors of the Cx-y catalysts (x, y, weight % of Pd and Bi loaded on resin) were prepared at laboratory temperature by the ion-exchange method according to reactions (1) and (2):

$$2\ (P)\text{-}N(CH_3)_3^+Cl^-\ (s) + [PdCl_4]^{2-} \rightarrow [(P)\text{-}N(CH_3)_3^+]_2[PdCl_4]^{2-}\ (s) + 2\ Cl^- \quad (1)$$

$$(P)\text{-}N(CH_3)_3^+Cl^-\ (s) + [BiCl_4]^- \rightarrow [(P)\text{-}N(CH_3)_3^+][BiCl_4]^-\ (s) + Cl^- \quad (2)$$

Defined amount of $PdCl_2$ and $BiCl_3$ dissolved in 10 mL of 4 M aqueous HCl were slightly stirred with the washed dried resin (3 g) for 4 h to give dark orange resin beads. Afterwards, the resin beads were separated from solution by filtration on a frit, washed with water until the chloride test was negative and dried at 50°C under reduced pressure to constant weight. The metallated resins (0.3 g) were reduced either with 1M solution of sodium borohydride (5 mL) in a mixture of isopropyl alcohol : water = 1 : 1 (vol.) (20 mL) or by bubbling with hydrogen (flow rate 20 mL per min) through 0.01 M aqueous sodium carbonate both procedures for 1 h at laboratory temperature. The as prepared catalysts were filtered, washed with a solution of isopropyl alcohol : water = 1 : 1 (vol.) (40 mL) and thus was directly used for the reaction. Borohydride reduced catalysts are referred to as Cx-yB and hydrogen reduced as Cx-yH. Actual metal loading of the catalysts are listed in Table 1.

Table 1 Actual metal content and particle size of the Pd-Bi/Dowex®1x4 catalysts

| | Loading [a] | | Pd size [b] |
|---|---|---|---|
| | Pd | Bi | (nm) |
| C3-1H | 2.9 | 1.1 | 5.5 |
| C3-1B | 2.9 | 1.1 | 3.4 |
| C3-03B | 2.9 | 0.3 | 3.9 |
| C3-05B | 2.8 | 0.6 | 3.8 |
| C3-3B | 2.8 | 3.1 | 3.4 |
| C3-45B | 2.7 | 4.6 | 2.9 |
| C2-06B | 2.1 | 0.6 | 2.6 |
| C1-03B | 1.0 | 0.3 | 2.8 |

[a] Weight % of Pd and Bi detected by AES-ICP and AAS-F methods, respectively
[b] Average diameter of Pd particles determined from XRD analysis for the half-with of the main Pd peaks corresponding to the (1 1 1) reflection

*2.3. Catalysts characterization*

The Pd and Bi loading was determined by inductively coupled plasma atomic emission spectroscopy (ICP AES) and flame atomic absorption spectroscopy (AAS-F), respectively using a Varian ICP-AES Spectrometers Varian 720-ES and Agilent DUO AA 240Z/240FS analyzer. Samples (ca. 0.5 g) were put in a Quartz crucible and kept in an incinerator at 600°C for 12 h. The black ash was dissolved in aqua, digested for 10 min and diluted using distilled water. X-ray powder diffraction analysis was performed using $CoK_{\alpha 1}$ radiation on Philips PW 1730/1050 diffractometer in the range of 7°-80°$2\Theta$ (scan time 2 s $step^{-1}$) and the diffractograms were compared to the JCDS-ICDD references. The metal particle size of the reduced and dried catalysts was determined using the Scherrer equation:

$$d_{Pd} = \frac{k.\lambda}{\beta.\cos(\Theta)}$$

with $d_{Pd}$ the mean size of the crystalline domains, $k$ (0.9) the shape factor, $\lambda$ (1.7902 Å) the wavelength, $\beta$ the line broadening at half the maximum intensity (FWHM) in radians and $\Theta$ the Bragg angle. The FT IR spectra of the dried samples in a wavenumber range of 4000–550 $cm^{-1}$ were obtained using the Shimadzu IRAffinity-1 spectrometer equipped with ATR technique. The UV-Vis spectrophotometer Shimadzu UV-2600 was used to determine the concentration of unanchored palladium(II) into the support during the ion-exchange reaction by iodide method [56]. The iodine method is based on the reaction of palladium(II) in an excess of KI to form a red-brown complex of $[PdI_4]^{2-}$ which is measured at the wavelength $\lambda_{max}$ 407 nm. The samples of Pd(II) with unknown concentration were prepared by addition of 5 mL of 6 M HCl, 10 $cm^3$ of 20 % KI solution, with 2 mL of 1 % ascorbic acid and 2 mL of chloride solution of Pd(II) taken from the ion-exchange. The solution was diluted with distilled water and the absorbance of Pd(II) was measured in the one-centimeter cell against blank test as the reference. The concentration of Pd(II) was determined on the base of calibration with known concentrations of Pd(II). Scanning electron microscopy (SEM) images were measured on a JEOL JSM-7500F microscope operated at accelerating voltages of 1 and 4 kV. Transmission electron microscopy (TEM) analysis was carried out with a JEM 3010 (JEOL) electron microscope operating at 300 kV, with the Lens parameters Cs = 0.6 mm and Cc = 1.3 mm, giving a point resolution of 0.17 nm at Scherzer defocus. X-ray photoelectron spectra (XPS) were measured on a Thermo Scientific K-Alpha XPS spectrometer fitted with X-ray monochromatized Al Kα radiation 12 kV, 6 mA.

*2.4. Catalyst testing*

The glycerol oxidation experiments were carried out under atmospheric pressure in a temperature-controlled 75 mL semi-batch glass reactor equipped with a magnetic stirrer, inlet for nitrogen or oxygen and pH-meter (Precision Digital pH meter OP-208/1, Hungary)

providing the continuous pH control during the reaction time. The reactions were performed with 50 mL of a 0.1 M aqueous glycerol solution at an oxygen flow rate of 200 mL $min^{-1}$ checked by mass flow controller; in temperature range from 35 to 50°C and a stirring rate of 100 - 700 rounds per minute (rpm). Reactions were carried out at constant pH (11 ± 0.3) regulated by addition of an aqueous solution of 40 % NaOH. During heating the reaction mixture was continuously flushed with nitrogen. The reaction started by switching the gas to oxygen.

The quantitative analyses of the reaction mixtures were performed on a high performance liquid chromatograph (Shimadzu, Japan) equipped with a SPD 10AVp and RID-10A detectors. An Aminex HPX-87H column (300x7.8 mm) was used with 0.008 N aqueous $H_2SO_4$ as eluent with a flow-rate of 0.5 mL $min^{-1}$. Samples of the reaction mixtures were diluted in the used eluent. Products were determined by external standard method with known concentration of commercial standards, after obtaining the calibration curves. Performance of the catalysts was evaluated in term of (%) conversion of glycerol and (%) selectivity to glyceric acid and tartronic acids calculated on the amount of converted glycerol. In the case of C1 and C2 products the selectivity was determined taking into account the carbon atom number of glycerol and the corresponding compounds.

The conversion was determined by the change in the concentration of glycerol within a period of time:

$$x_{GLY} = \frac{m^0_{GLY} - m^t_{GLY}}{m^t_{GLY}} \cdot 100$$

where $x_{GLY}$ is the glycerol conversion; $m^0_{GLY}$ is the glycerol initial molar concentration and $m^t_{GLY}$ is the glycerol molar concentration at *t* time.

The selectivity of compound *i* was determined according to equation:

$$S_i = \frac{m^t_i}{(m^0_{GLY} - m^t_{GLY})} \cdot \frac{CAN_i}{3}$$

where $m^t_i$ is the molar concentration of compound *i* at time *t and* $CAN_i$ is the carbon atoms number of the corresponding compound.

*2.5. Catalyst recycling experiments*

A typical recycling experiment was carried out as follows: After the reaction with fresh catalyst, the content of the reactor (suspension of the catalyst with the reaction mixture) was cooled to laboratory temperature, sealed and stored in a refrigerator. The next day, the catalytic resin was separated from the reaction mixture by simple filtration on a frit S4. Then the catalyst was washed on a frit with 2x20 mL solution of isopropyl alcohol : water = 1 : 1 (vol.) and was directly used for the next run of reaction with a fresh reactants. Experiments were performed at 50°C for three hours.

## 3. Results and discussion

*3.1 Catalysts preparation and characterization studies*

The commercially available gel-type strong anion-exchange resin Dowex®1x4 in chloride form on the base of poly(styrene-*co*-divinylbenzene) which contains trimethylbenzyl ammonium functionalities (0.396 mmol per 100 mg of resin, N-content of 5.54 wt. %) was used to support Pd-Bi-nanoparticles (Pd-Bi-NPs).

Preliminary study showed that the method of Pd and Bi introduction order (simultaneous or sequential) and reduction procedure (final or sequential) have significant influence on the catalytic performance. Precursors of the catalysts prepared and reduced by sequential steps had low activity and selectivity. Better conversion and selectivity to target acids was obtained when only the catalysts precursors were prepared by sequential loadings and reduced to the end in one step. Enhanced glycerol conversion and high selectivity to target acids exhibited the catalysts where the metal precursors were added simultaneously to the resin and followed the final reduction. This suggests that the arrangement of the metal species may play a key role on the catalytic performance. Scheme 1 shows the synthesis procedure.

The synthesis of Pd-Bi-NPs stabilized within the gel-type anion-exchange resin comprised of the partial exchange of $Cl^-$ to the $PdCl_4^{2-}$ and $BiCl_4^-$ (Scheme 1, a) and followed by the rapid reduction of the anchored anionic Pd(II)-Bi(III) compound either with $NaBH_4$ in a solution of isopropyl alcohol and water (vol. 1:1) or molecular hydrogen in an aqueous solution of $Na_2CO_3$ (0.01 M) (Scheme 1, b). The evolution of the Pd(II) ions content in the solution after the ion exchange reaction was monitored by UV Vis spectrophotometric methods [56]. The reduction of the content of Pd(II) ions in the solution means that the Pd(II) were anchored into the resin. In preparing the bimetallic C3-1 precursor, the ion-exchanged amount of Pd(II) ions reached 85.1 %, 88.4 %, 89.0 % and 88.9 % for the ion-exchange times of 2, 3, 4 and 20 h, respectively, indicating that the ion-exchange process is very fast at the initial stage and the ion-exchange process tend to reach a saturation state after stirring for 4 h (Fig. 1). When the C1-03 precursor was prepared, the ion-exchanged amount of Pd(II) ions reached 99.0 % after 4 h. In the case of $BiCl_4^-$ ions, after 4 h the ion exchange reaction was practically total at the bimetallic compositions in the used concentration interval of bismuth (0.3 - 4.5 wt. %). Therefore, all catalysts were prepared by stirring for 4 h.

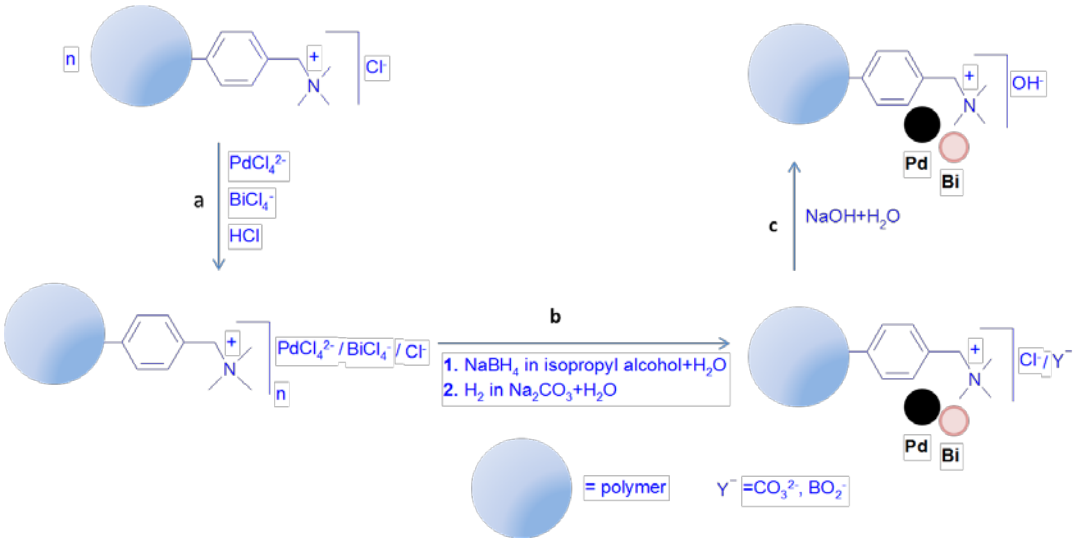


Scheme 1 Synthesis of Pd-Bi-NPs stabilized by Dowex®1x4

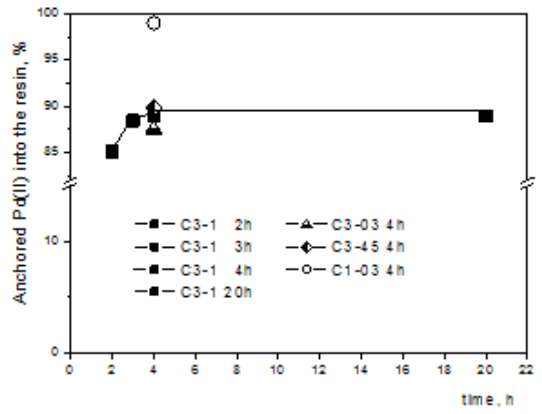


Fig. 1 Anchored amount of Pd(II) ions into the resin during the ion-exchange reaction

Variations of absorption bands in the infrared spectrum of the resin after ion-exchange reaction of $Cl^-$ for $PdCl_4^{2-}$ and $BiCl_4^-$ (step "a" in the scheme 1) are negligible (Figs. 2a-b). Depending on the degree of washing, after reduction (step "b"), the presence of carbonate or borate counter ions can be recognized in the reflection IR spectra (Figs. 2c-d). However, treatment of the Pd-Bi containing resins with an aqueous solution of NaOH (step "c") immediately yielded the corresponding resin in its hydroxyl form, such as it is present in the reaction mixture (Figs. 2e-f). Adjustment of the resin itself with an aqueous solution of NaOH results in the same changes in the IR spectrum, as seen in Fig. 2g.

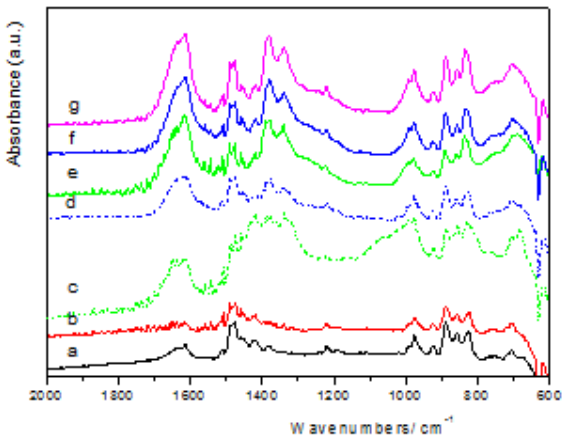


Fig. 2 Infrared spectra of dried Dowex1x4 (a), precursor of C3-1 catalyst (b), catalysts C3-1B (c), C3-1H (d), C3-1B+NaOH (e), C3-1H+NaOH (f) and Dowex1x4+NaOH (g)

X-ray diffraction analysis of all catalysts reduced either by $NaBH_4$ or hydrogen exhibited predominantly the presence of (1 1 1) reflections assigned to the face-centered cubic *(fcc)* unit cell of metallic palladium, confirm the crystalline nature of the particles (Fig. 3). In some patterns the small peak assigned to the Pd (2 0 0) plane was found; however, the reflection of others planes was not observed, suggesting the presence of small Pd particles. None of the monoclinic, orthorhombic, rhombohedral unit cell related to the known $Pd_x$-$Bi_y$ compounds (where x = 1 – 31 and y = 1 – 12) were recorded in the bimetallic Pd-Bi catalysts. Except the C3-45B composition, neither characteristic crystalline phase for single bismuth species was shown in the patterns. In the spectrum of the C3-45B catalyst, a broad diffraction peak corresponding to α-$Bi_2O_3$ (JCPDS No. 41-1449) was recognized (Fig. 3B). Interesting was the finding that the C3-1H catalyst presents an obvious shift of the diffraction peak of Pd (1 1 1) towards higher $2\Theta$ values which may be caused by insetting of bismuth into the Pd crystal lattice. Cai et al. [57] have similar report for bimetallic Pd-Bi/C catalyst. In the case of borohydride reduced catalysts the average diameter of the palladium particles estimated from the diffraction peak of (1 1 1) according to the Scherrer formula was found to be in the range of 3.9 to 2.6 nm (Table 1) and the average diameter of 4.6 nm for the α-$Bi_2O_3$ particles in the C3-45B composition. The results indicate that the particle size of Pd crystallites does not significantly depend on the amount of Pd loaded in the range of 1 – 3 wt. %. However, lower portion of Bi to Pd (0.3÷0.5Bi/3Pd) causes that the Pd particles remain slightly larger (3.8-3.9 nm) than those with higher content of Bi (3.4-2.6 nm). The most probably explanation for this phenomenon is a so called „ensemble effect“, when the Bi promotor located on a fraction of active metal sites decreases the size of noble metal ensembles [36,38-40]. On the other hand, the particle sizes of Pd 5.5 nm were significantly higher using hydrogen as reducing agent.

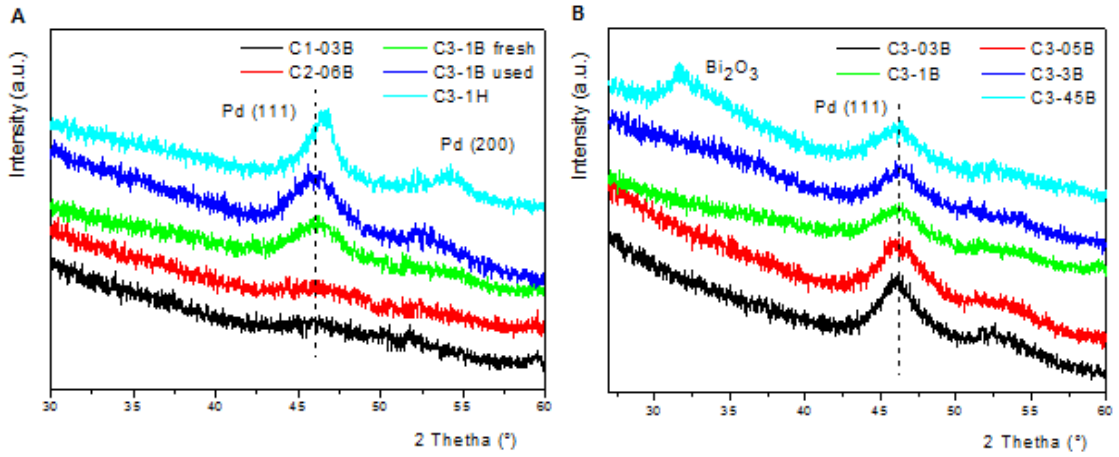


Fig. 3 XRD patterns of Pd-Bi/Dowex1x4 catalysts with varying amounts of deposited metal reduced in two ways (A) and a different weight ratio of Bi and Pd (B). Crystalline phases of Pd and α-$Bi_2O_3$ were identified according to JCPDS Card No. 05-0681 and 76-1730, respectively.

TEM pictures of C3-1H and C3-1B catalysts are shown in Fig. 4. The picture of Fig. 4A proves the size of Pd crystallites in the C3-1H catalyst corresponds with the result of XRD technique. Comparing with the C3-1H catalyst, the size of Pd particles look smaller in the C3-1B catalyst recorded in Fig. 4B, however, their dimension cannot be unambiguously estimated since several particles are interconnected.

SEM measurement was used to investigate the morphology of selected catalysts (Fig.5). Focus on one bead brought finding that metallic particles are distributed on the outside and the inside of the resin. Figs. 5A and 5B reveal that in the surface of both catalysts the distribution of metallic particles are quite homogeneous, however, the coverage of the outer surface of the C3-1H catalyst reduced with hydrogen is clearly higher than in the case of the borohydride reduced C3-1B composition. The proportion of metal particles located on the outer layer of the beads decreases significantly with decreasing amount of deposited metals. On the external surface of C2-06B and C1-03B catalysts with lower metal contents merely very few metallic particles were observed (Fig. 5C and 5D). This indicates that the metallic particles are concentrated predominantly in the inner part of the resin. The particles on the surface are clustered into larger agglomerates (units). This may be related to the unlimited space available on the surface. Interestingly, these more dense populations of metallic particles form coral looks and roundish clusters for borohydride-reduced and hydrogen-reduced catalyst, respectively (Figs. 5E and 5F). In all cases, the agglomerates are composed of numerous small, so-called primary particles recognizable by TEM measurement (Fig. 4).

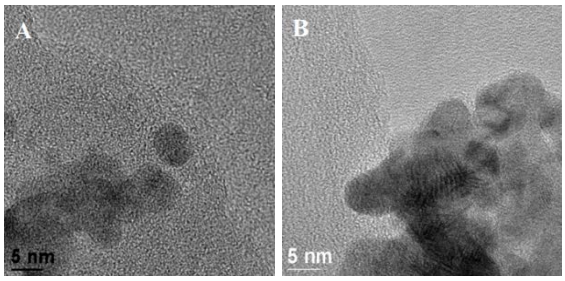


Fig. 4 TEM images of C3-1H (A) and C3-1B (B) catalysts

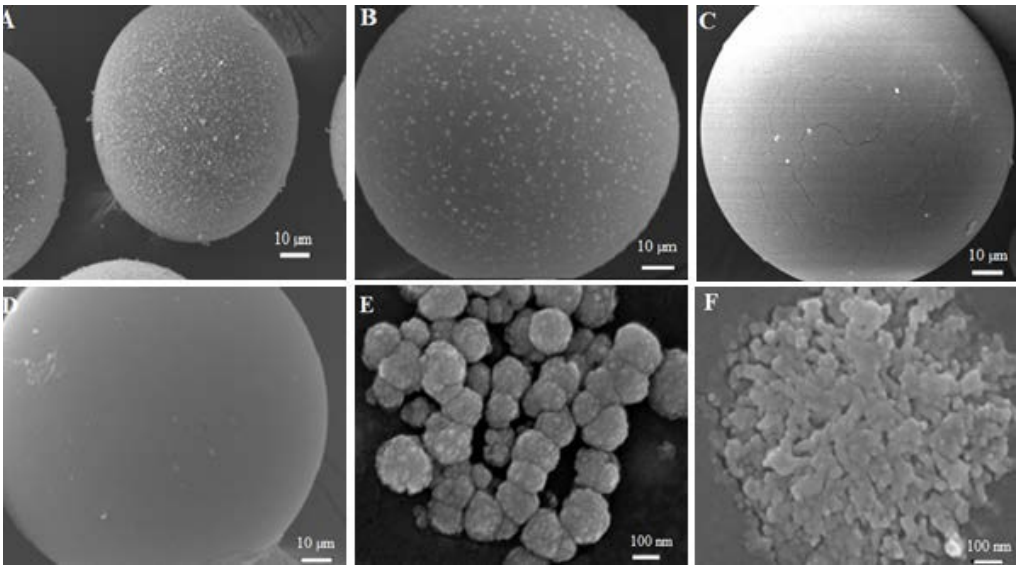


Fig. 5 SEM micrographs of the as prepared Pd-Bi containing Dowex®1x4 microparticles: focused on one bead of C3-1H (A), C3-1B (B), C2-06B (C) and C1-03B (D), surface morphology of C3-1H (E) and C3-1B (F) catalysts

The chemical states of the active phase in C3-1B and C3-1H catalysts were determined by XPS analysis and the spectra are recorded in the Fig. 6. Palladium and bismuth species appear in the metallic (Pd(0), Bi(0)) and the oxidized form (Pd(II), $Pd(II)_{ads}$, Bi(III)) [57]. The binding energy values associated with the Pd $3d_{5/2}$ photopeak, lie in the range 335.1-335.3 eV for Pd(0) and 338.3-338.6 eV for Pd(II), $Pd(II)_{ads}$ and for the Bi $4f_{7/2}$ line in the range 158.0-158.3 eV for Bi(0) and 164.0-164.3 eV for Bi(III). The experimental Bi/Pd atomic ratio calculated from XPS measurements for C3-1H catalyst (~ 0.17) is very similar to the theoretical value obtained from the bulk composition. In the case of C3-1B, the experimental Bi/Pd atomic ratio (~ 0.77) is higher than that for the bulk catalyst, therefore suggests a partial coverage of palladium with bismuth. Another possible explanation of this phenomenon is a diffusion of metallic bismuth towards the external surface of the active phase by the reason of

its lower surface energy compared to palladium [52]. In view of the same bulk composition of both compared catalysts which can provide the same environment for the diffusion through the material, the coverage of Pd by Bi in line with the literature results seems to be more likely in our case [30,31]. The results may explain the different spatial configuration of the metallic particles observed in the SEM pictures for both the compared catalysts (Figs.5E and F). It should be taken into account that after initial reduction with borohydride or in hydrogen atmosphere, the catalysts were in contact with air and were not reduced immediately prior to the XPS analysis, what may contribute to the presence of the oxidized form of palladium and bismuth.

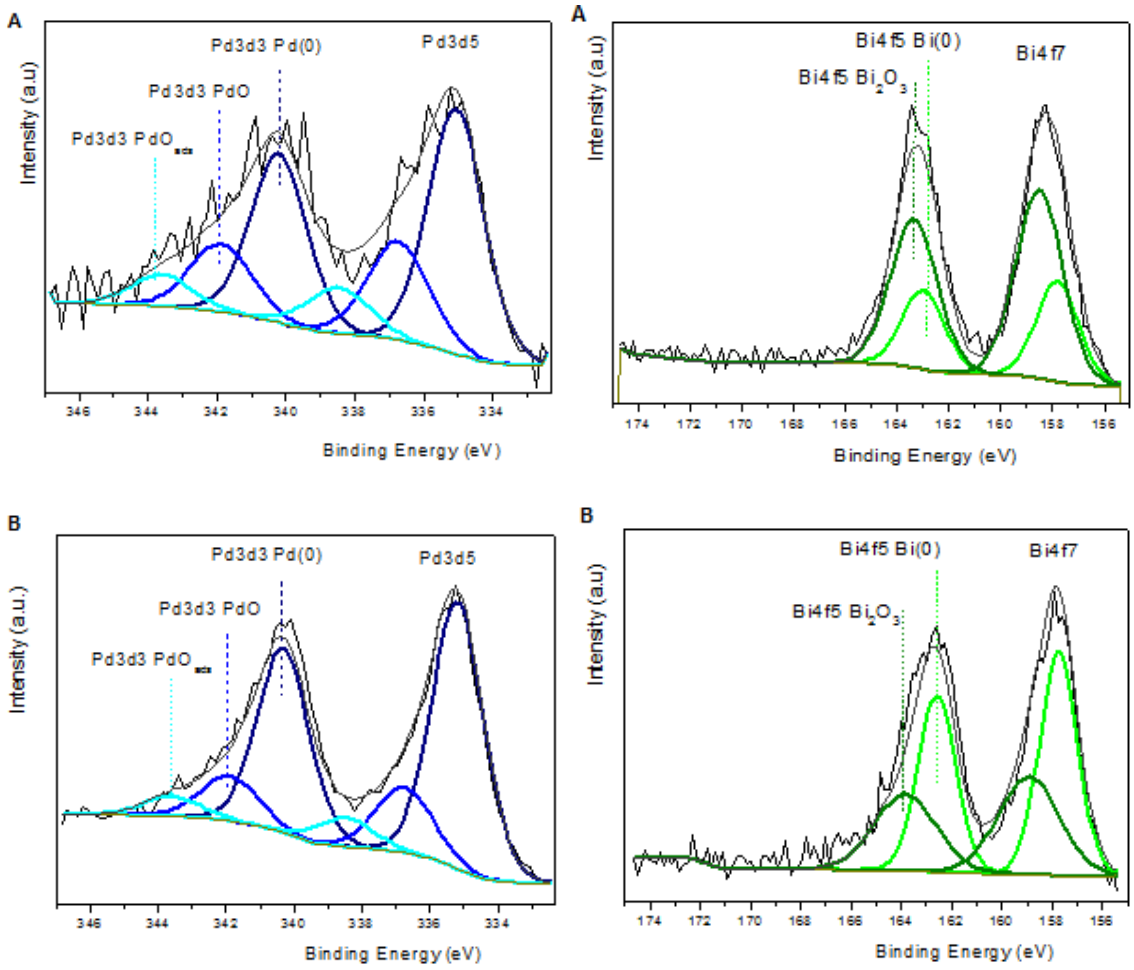


Fig. 6 XPS spectra of C3-1B (A) and C3-1H (B) catalysts in Pd 3d and Bi 4f regions

*3.2 Catalytic performance*

Liquid phase oxidation of glycerol was studied in a batch reactor at atmospheric pressure. Properties of the catalysts were compared with an oxygen flow rate of 200 mL $min^{-1}$ and under basic conditions (pH 11 ± 0.3). Without addition of a base, the pH of the reaction mixture decreased rapidly from an initial value of 7.6 to 3 within the first hour of the reaction

and would not change eventually. At 15 % conversion of glycerol, the reaction product was in particular glyceric acid; however, the selectivity to dihydroxyacetone (a typical product being formed in acidic medium) did not exceed the level 0.1 %. Since, neither conversion nor selectivity did change even after 8 hours of reaction; nonetheless this path would not be further invesigated. The influence of stirring speed in the range of 100-700 rpm at 50°C using C3-1B catalyst was examined. The results showed that the respective initial reaction rates increase from 28 to 78 mmol $L^{-1}$ $h^{-1}$ in the range from 100 to 400 rpm. Above 400 rpm, the gain on the initial reaction rates was negligible and the selectivity to glyceric acid persisted with relatively little change. Based on these characteristics, the stirring speed of 400 rpm was chosen. In a previous experiment was proved that the polymeric resin Dowex1x4 itself without presence of metal particles is inactive for the liquid phase transformation of glycerol.

Fig. 7 shows the activity of C3-1B and C3-1H catalysts in terms of glycerol conversion and glyceric acid and tartronic acid selectivity as a function of time whereas Table 2 lists the products selectivity. The main reaction products determined after glycerol oxidation were glyceric acid (GLYA) and tartronic acid (TARA), but glycolic acid (GLYCA) and minor amounts of formic acid (FORMA) and oxalic acid (OXA) were also formed. In the initial stages of the reaction, especially at low temperature and a lower metal content glyceric aldehyde could be observed among the reaction products. However, due to its instability in acid solution, wherein the analysis was made, the quantification failed. The interconversion of glyceric aldehyde to dihydroxyacetone depending on the acid-base character of the reaction medium is reported in [3]. In the presence of borohydride reduced catalyst more than 1.5 times higher initial rate of glycerol oxidation was reached than over the catalyst reduced by hydrogen (78 *vs.* 51 mmol $L^{-1}$ $h^{-1}$ calculated after first 0.5 h of the reaction). The selectivity to glyceric acid was also higher over C3-1B catalyst compared to C3-1H composition (69 % *vs.* 59 % at 50 % conversion of glycerol), but the selectivity to tartronic acid was almost the same. This was surprising; since on the basis of the SEM images (Figs.5A and 5B) we expected that the catalyst containing a higher number of metal particles on the outside would be more active than the one with lower coverage. A possible explanation could indicate that not only the particles on the external surface but also those in the swelling gel phase of the copolymeric matrix may play an important role in the oxidation reaction. On the other hand, the different catalytic activity may be associated with a different arrangement of Pd and Bi particles as well as with a slightly different particle size of metals. As explained in the XPS analysis, the Bi promoter is deposited on the surface of the Pd particles in the C3-1B catalyst, which in accordance with previous findings reported for Pd-Bi/C catalysts i) has a beneficial effect on the rate of oxidation reaction [36] and ii) improve the selectivity of the product formation [38]. In the case of C3-1H composition, bismuth is located near the palladium particles, even slightly deforms the crystal lattice, as shown by the XRD analysis. An important parameter widely discussed in literature is particle size of metals which significantly affects the activity of the catalysts in the glycerol oxidation. Due to the fact that the particle size of Pd in C3-1B catalyst is smaller than that in the C3-1H composition (3.4 nm and 5.5 nm, respectively), this may also contribute to a difference in the catalytic performance. The results are in agreement with various studies of carbon or $TiO_2$ supported Pd as well as Au catalysts in terms of catalytic activity, because small particles exhibit higher

catalytic activity [15-19]. The selectivity is not directly correlated to the size of nanoparticles. Several authors have found that larger metal particles are more selective in glycerol liquid phase oxidation. However, Gil et al. [22] reported for gold-sol supported catalyst that both conversion and selectivity increased with decreasing gold particle sizes, what is in good agreement in our experimental results.

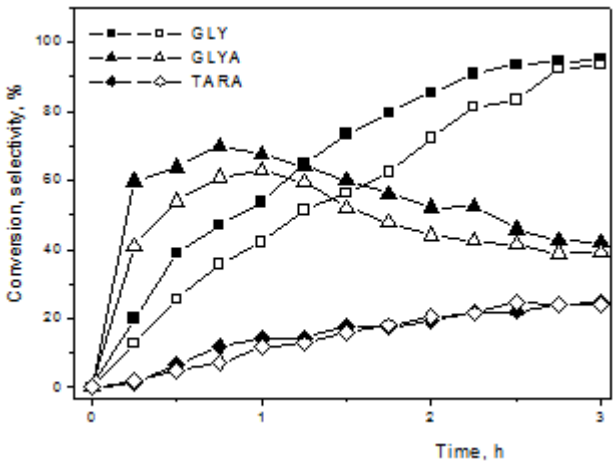


Fig. 7 Catalytic performance of Pd-Bi nanoparticles reduced with borohydride and hydrogen in C3-1B and C3-1H catalysts. Reaction conditions: 0.3 g of catalyst, initial concentration of glycerol 0.1 mol $L^{-1}$, 50°C, pH 11, stirring speed 400 rpm, oxygen flow-rate 200 mL $min^{-1}$, atmospheric pressure. Symbols: full - C3-1B and open - C3-1H catalysts

Table 2 Influence of reduction methods and amount of metals loaded on catalytic performance of Pd-Bi-NPs stabilized within Dowex 1x4 [a]

| | $r_{init}$ [b] | $t_{50}$ [c] (min) | $X_{GLY}$ [d] (%) | Selectivity [e] (%) | | | | | Y [f] (%) |
|---|---|---|---|---|---|---|---|---|---|
| | | | | GLYA | TARA | GLYCA | FORMA | OXA | GLYA+TARA |
| C3-1H | 51 | 75 | 93 | 59 | 14 | 6 | 7 | 2.2 | 59 |
| C3-1B | 78 | 50 | 95 | 68 | 15 | 4 | 10 | 1.1 | 63 |
| C2-06B | 42 | 100 | 68 | 59 | 14 | 10 | 4 | 1.1 | 48 |
| C1-03B | 25 | 260 | 47 | 51 | 14 | 12 | 2 | 1.1 | 29 |

[a] – Reaction conditions: as seen in Fig. 7, [b] – Initial reaction rate (mmol $L^{1-}$ $h^{1-}$) determined after 0.5 h of reaction, [c] – reaction time to achieve 50 % glycerol conversion, [d] – conversion of glycerol after 3 h of reaction, [e] – selectivity to glyceric acid (GLYA), tartronic acid (TARA), glycolic acid (GLYCA), formic acid (FORMA) and oxalic acid (OXA), respectively at 50 % of glycerol conversion, [f] – yield of Σ(glyceric acid and tartronic acid) after 3 h of reaction.

To elucidate the amount of bismuth on the performance of the catalysts, the ratio of Pd and Bi keeping the amount of Pd constant at a 3 wt. % by varying the content of Bi in the range from

0.3 to 4.5 wt. % was studied. Earlier experiments have shown that bismuth deposited alone into the resin (1 wt. %) is inactive and in the presence of a catalyst containing palladium alone (3 wt. %) the glycerol conversion reaches up to 19 % after four hours of reaction. Synergic effect between Pd and Bi for glyoxal or glucose oxidation is known from literature [15,31,37-39], however, the improved properties of Bi-doped Pd catalyst supported on carbon was not confirmed for glycerol oxidation to glyceric acid in [14]. In our case, the increasing Bi content from 0.3 to 1 wt. % enhances the glycerol conversion from 56 to 95 % (Fig. 8). Further increase in the Bi practically does not change the catalysts activity. Above this value, the selectivity to glyceric acid gradually decreases and the selectivity of tartronic acid almost does not alter (reaches around 20 %). This suggests that in accordance to literature data [36,38-40], blocking of various fractions of the active palladium species with bismuth provides different substrate coordination and in turn modifies the selectivity to glyceric acid. It seems that separated bismuth oxide species present in the C3-45B catalyst do not influence the catalytic performance; they appear to be only „spectators".

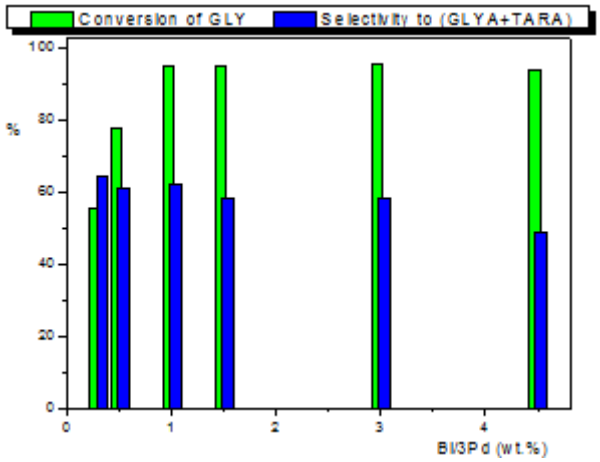


Fig. 8 Influence of the Bi-Pd ratio on glycerol conversion and selectivity to sum of glyceric acid and tartronic acid after three hours of reaction. Reaction conditions: as seen in Fig.7.

Comparing the content of palladium loaded into the polymeric matrix (Table 2) it was found that increasing the metal content from 1 to 3 wt. % results in i) an increasing the initial rate of glycerol transformation (from 25 to 78 mmol $L^{-1}$ $h^{-1}$ calculated after 0.5 h of reaction), ii) thus shortening of the time to reach the glycerol conversion of 50 % from 260 to 50 min and iii) the latter suppresses the overoxidation associated with the cleavage of the C-C bond yielding C2 and C1 products and thereby increasing the yield of target products from 29 to 63 % calculated after 3 hours of the reaction. It would be valuable noted that increase of the Pd content in the prepared catalysts from 1 to 3 wt. % varies in particle size in the range of 2.3-3.4 nm, which allows to compare primarily the contents of metals in the catalysts.

In order to get further information on the properties of the catalysts, the influence of reaction temperature on the rate of glycerol oxidation at temperatures from 35 to 50°C in the presence

of C3-1B catalysts was studied (Fig. 9A). The results allow determining the initial reaction rates for different temperatures. Fig. 9B shows the calculated initial reaction rates obtained after the first 30 minutes of the reaction as a function of the reciprocal value of the reaction temperature. From these data the apparent activation energy of the C3-1B catalyzed liquid phase oxidation of glycerol could be estimated to 44±5 kJ/mol. The value is very similar as that one calculated for the carbon supported gold catalyzed glycerol oxidation (50±5 kJ/mol) [18, 59].

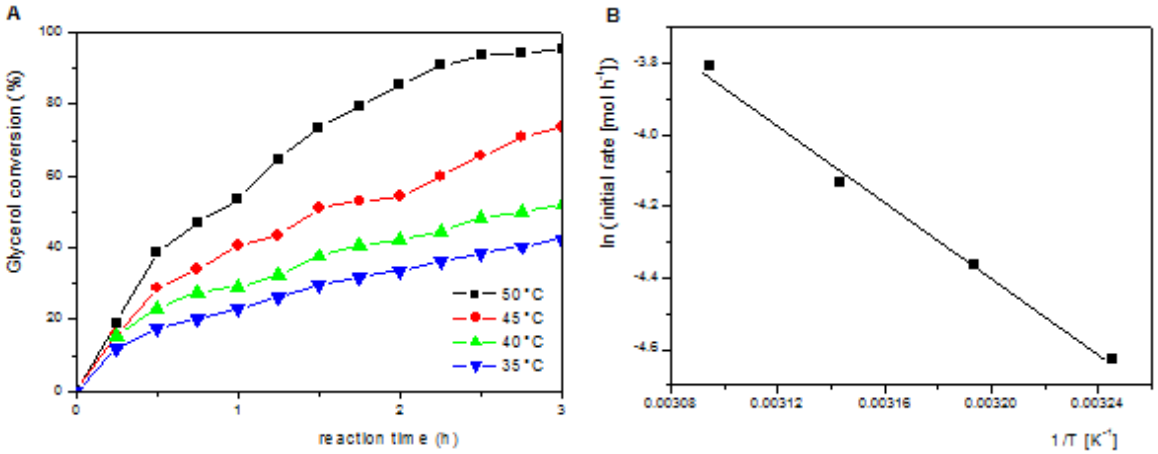


Fig. 9 Variation of glycerol conversion as a function of time at different temperatures (A) and the Arrhenius plot of the initial reaction rates (B) both caused by the catalysts C3-1B

The recyclability and recoverability of Pd-Bi nanoparticles are investigated through a five-run recycling test of glycerol oxidation in the presence of C3-1B catalyst (Fig. 10). There are little fluctuations in the glycerol conversion during the incipient four recycling runs. At that time, the overall selectivity to glyceric acid and tartronic acid, two consecutive products, increases gradually from 63 % to 80 %. The polymeric matrix stabilized Pd-Bi nanoparticles maintains more than 90 % of their initial catalytic activity at the end of the fifths cycle calculated from the glycerol conversion. After that run, the overall selectivity of both target products reached 73 %. Metal sintering and/or leaching are known reasons for noble metal catalysts deactivation in liquid phase oxidation reactions of alcohols [37-39]. After second catalytic run, the concentration of dissolved palladium and bismuth species in the reaction mixture was detected by ICP OES and AAS-F. The bismuth concentration was 0.05 wt. % (calculated on the deposited amount) and the leached palladium was negligible. The XRD analysis indicated that the size of palladium particles was with almost no change; it was 3.4 nm for the fresh catalyst and 3.5 nm after the fifth recycling test (Fig. 3, C3-1B used). Possible reason for the decrease in activity in this case can be attributed to a loss in handling between different experiments. These findings could support the assumption that the swollen gel phase of the

used resin facilitates completing the reaction cycle inside the copolymeric matrix and mitigate the metals leaching during mass transfer between the catalysts and the reaction solution [60].

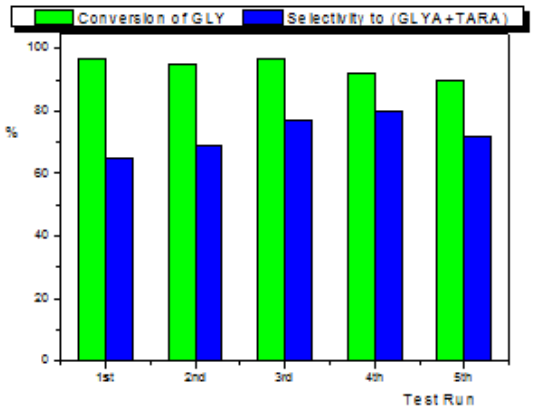


Fig. 10 The five-run recycling test of glycerol oxidation over C3-1B catalyst. Reaction conditions: as seen in Fig. 7.

The mechanism of liquid phase oxidation of glycerol in a basic medium using molecular oxygen in the presence of supported monometallic or bimetallic Au-, Pd- or Pt-based catalysts proceeds via subsequent oxidation reactions as is reported in the literature [23,26-28]. The reaction pathway of glycerol oxidation involves the formation of glyceraldehyde in the initial stage of the reaction which is oxidized to glyceric acid and in the next step to tartronic acid. Decarboxylation of tartronic acid yields glycolic acid. Similarly as in our case, the formation of a less obvious formic acid was observed by the authors of gold supported catalysts in [26,27]. The origin of formic acid suggested in [26] assumes that the initially formed glyceric acid undergoes to a reverse-aldol rearrangement to give glycolic acid and formaldehyde, where the latter is readily oxidized to formic acid. The possible reaction pathways for the partial oxidation of glycerol with Pd-Bi/Dowex®1x4 catalysts are depicted in Scheme 2.

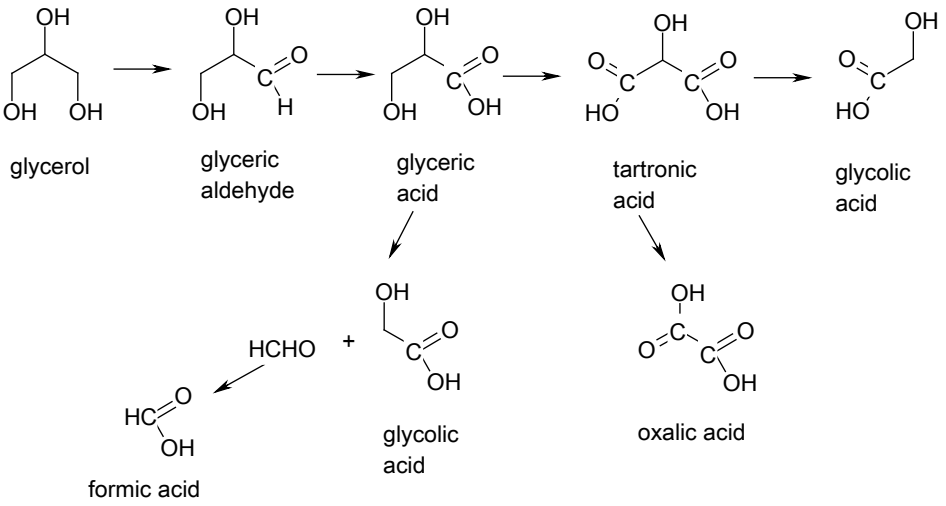


Scheme 2 Possible reaction pathways for glycerol oxidation over Pd-Bi/Dowex®1x4 catalyst

## 4. Conclusions

We have shown that palladium bismuth nanoparticles stabilized within well-defined gel-type strong anion-exchange resin can easily be prepared by ion-exchange method and serve as efficient, recyclable catalyst for glycerol oxidation with molecular oxygen under mild reaction conditions (at 35-50°C and atmospheric pressure). We have demonstrated that the direct ion-exchange reaction leading to the formation of the catalysts precursors tends to reach a fast saturation, moreover, the Pd-Bi surface configuration as well as the size of Pd particles is altered by reduction method used.

It has been observed that in comparison with the catalyst reduced by hydrogen; the catalysts prepared by borohydride reduction exhibited better catalytic performance. It was associated with i) the smaller size (2.6-3.4 nm, *vs.* 5.5 nm) of crystalline particles of active palladium species even when the loading was in the relatively broad range of 1-3 wt. % and ii) also by the different configuration of the palladium and bismuth species. We ascribed that mainly the geometric effect when Bi were deposited on Pd species provided preferable substrate coordination routes which could be responsible for the more than 1.5 times higher initial reaction rate of glycerol. In terms of the yield of target products (glyceric acid and tartronic acid) the catalysts with different Pd/Bi configurations did not show significant variations (63% *vs*. 59%). This enables to conclude that given the proximity of bismuth and palladium species in both systems, the electronic effect might be active in modifying the selectivity. We assume that swollen gel phase of the resin used as a support is responsible for the possibility of re-using the catalyst (3%Pd-1%Bi, $d_{Pd}$=3.4 nm) at least five catalytic cycles practically with a similar catalytic performance as of the fresh catalyst by only washing with isopropyl alcohol-water after each run.

**Acknowledgements**

This work was financially supported by Scientific Grant Agency of the Slovak Republic under the project No. Vega 1/0556/13 and by the Slovak Research and Development Agency under the contract APVV-0133-11.

## References

[1] O.R.Inderwildi, D.A. King, Quo vadis biofuels?, Energy Environ. Sci 2 (2009) 343-346.
[2] M. Pagliano, M. Rossi, The future of glycerol, 2nd edn. (RSC Green Chemistry Book Series) 2010.
[3] B. Katryniok, H. Kimura, E. Skryńska, J.S. Girardon, P. Fongarland, M. Capron, R. Ducolumbier, N. Mimura, S. Paul, F. Dueignil, Green Chem. 13 (2011) 1960.
[4] Y. Zheng, X. Chen, Y. Shen, Chem. Rev. 108 (2008) 5253.
[5] Z. Liu, J. Wang, M. Kang, N. Yin, X. Wang, J. Ind. Eng. Chem. 21 (2015) 394.
[6] L. Shen, H. Yin, A. Wang, X. Lu, C. Zhang, F. Chen, Y. Wang, H. Chen, J. Ind. Eng. Chem. 20 (2014) 759.
[7] H. Rastegari, H.S. Ghaziaskar, J. Ind. Eng. Chem. 21 (2015) 856.
[8] P.S. Reddy, P. Sudarsanam, B. Mallesham, G. Raju, B.M. Reddy, J. Ind. Eng. Chem. 17 (2011) 377.
[9] S.E. Davis, M.S. Ide, R.J. Davis, Green Chem., 15 (2013) 17.
[10] H. Habe, T. Fukuoka, D. Kitamoto, K. Sakaki, Appl. Microbiol. Biotechnol. 84 (2009) 445.
[11] P. Fordham, M. Besson, P. Gallezot, Appl. Catal. A: Gen. 133 (1995) L179.
[12] H. Kimura, A. Kimura, I. Kokubo, T. Wakisaka, Y. Mitsuda, Appl. Catal. A: Gen. 95 (1993) 143.
[13] H. Kimura, Appl. Catal. A: Gen. 105 (1993) 147. [14] R. Garcia, M. Besson, P. Gallezot, Appl. Catal. A: Gen. 127 (1995) 165.
[15] P. Gallezot, Catal. Today 37 (1997) 405.
[16] S. Carrettin, P. McMorn, P. Johnston, K. Griffin, C. J. Kiely, G.J. Hutchings, Phys. Chem. Chem. Phys. 5 (2003) 1329.
[17] F. Porta, L. Prati, J. Catal. 224 (2004) 397.
[18] S. Demirel-Gülen, M. Lucas, P. Claus, Catal. Today 102–103 (2005) 166.
[19] S. Demirel, K. Lehnert, M. Lucas, P. Claus, Appl. Catal. B: Environ. 70 (2007) 637.
[20] D. Liang, J. Gao, J. H. Wang, P. Chen, Z. Y. Hou, X. M. Zheng, Catal. Commun. 10 (2009) 1586.
[21] J. Gao, D. Liang, P. Chen, Z. Hou, X. Zheng, Catal. Lett. 130 (2009) 185.
[22] S. Gil, L. Muñoz, L. Sánchez-Silva, A. Romero, J.L. Valverde, Chem. Eng. J. 172 (2011) 418.
[23] S. Gil, M. Marchena, L. Sánchez-Silva, A. Romero, P. Sánchez, J.L. Valverde, Chem. Eng. J. 178 (2011) 423.
[24] S. Demirel, K. Lehnert, M. Lucas, P. Claus, Catal. Today. 122 (2007) 292.
[25] N. Dimitratos, A. Villa, C.L. Bianchi, L. Prati, M. Makkee, Appl. Catal. A: Gen. 311 (2006) 185.

[26] N. Dimitratos, J.A. Lopez-Sanchez, J.M. Anthonykutty, G. Brett, A.F. Carley, R.C. Tiruvalam, A.A. Herzing, C.J. Kiely, D.W. Knight, G.J. Hutchings, Phys. Chem. Chem. Phys. 11 (2009) 4952.
[27] I. Sobczak, K. Jagodzinska, M. Ziolek, Catal. Today 158 (2010) 121.
[28] A. Villa, A. Gaiassi, I. Rossetti, C.L. Bianchi, K. van Benthem, G.M. Veith, L. Prati, J. Catal. 275 (2010) 108.
[29] A. Tsuji, K. Tirumala, V. Rao, S. Nishimura, A. Takagaki, K. Ebitani, ChemSusChem 4 (2011) 542.
[30] M. Besson, F. Lahmer, P. Gallezot, P. Fuertes, G. Fleche, J. Catal. 152 (1995) 116.
[31] M. Wenkin, P. Ruiz, B. Delmon, M. Devillers, J. Mol. Catal. A: Chem. 180 (2002) 141.
[32] C. Keresszegi, T. Mallat, J.D. Grunwaldt, A. Baiker, J. Catal. 225 (2004) 138.
[33] Mallat, Z. Bodnar, A. Baiker, Stud. Surf. Sci. Catal. 78 (1993) 377.
[34] S. Karski, I. Witońska, J. Mol. Catal. A: Chem. 191 (2003) 87.
[35] A. Villa, D. Wang, G.M. Veith, L. Prati, J. Catal. 292 (2012) 73.
[36] M. Besson, P. Gallezot, in R.A. Sheldon, H. van Bekkum (Eds.), Fine Chemicals through Heterogeneous Catalysis, Wiley-VCH, Weinheim, 2001, p.49
[37] T. Mallat, Z. Bodnar, A. Baiker, O. Greis, H. Strubig, A. Reller, J. Catal. 142 (1993) 237.
[38] T. Mallat, A. Baiker, Appl. Catal. A 79 (1991) 41.
[39] T. Mallat, Z. Bodnar, P. Hug, A. Baiker, J. Catal. 153 (1995) 131.
[40] C. Keresszegi, J.D. Grunwaldt, T. Mallat, A. Baiker, J. Catal., 222 (2004) 268.
[41] D.C. Sherrington, J. Polym. Sci. Part A: Polym. Chem. 39 (2001) 2364.
[42] M. Králik, A. Biffis, J. Mol. Catal. A: Chem. 177 (2001) 113.
[43] C. Burato, P. Centomo, G. Pace, M. Favaro, L. Prati, B. Corain, J. Mol. Catal. A: Chem. 238 (2005)26.
[44] A. Biffis, S. Cunial, P. Spontoni, L. Prati, J. Catal. 251 (2007) 1.
[45] F.H. Richter, Y. Meng, T. Klasen, L. Sahraoui, F. Schüth, J. Catal. 308 (2013) 341.
[46] R. Aikyama, S. Kobayashi, Chem. Rev. 109 (2009) 594.
[47] S. Gil, C. Jiménez-Borja, J. Martin-Campo, A. Romero, J.L. Valverde, L. Sánchez-Silva, J. Colloid Interface Sci. 431 (2014) 105.
[48] S. Gil, N. Cuenca, A. Romero, J. L. Valverde, L. Sánchez-Silva, Appl. Catal. A: Gen. 472 (2014) 11.
[49] A. Villa, C.E. Chan-Thaw, L. Prati, Appl. Catal. B: Environ. 96 (2010) 541.
[50] M.S. Gross, B.S. Sánchez, C.A. Querini, Appl Catal A: Gen. 501 (2015) 1.
[51] N. Mimura, N. Hiyoshi, T. Fujitani, F. Dumeignil, RSC Adv. 4 (2014) 33416.
[52] Kirk-Othmer, Encyclopedia of Chemical Technology, 4th Edition, John Wiley & Sons., 2006.
[53] M.D. Victor-Ortega, J.M. Ochando-Pulido, D.Airado-Rodrígeuez, A. Martínez-Ferez, J. Ind. Eng. Chem. 34 (2016) 224.
[54] T. Nur, M.A.H. Johin, P. Loganathan, T. Nguyen, S. Vigneswaran, J. Kandasamy, Ind. Eng. Chem. 20 (2014) 1301.
[55] A. Biffis, N. Orlandi, B. Corain, Adv. Mater. 15 (2003) 1551.
[56] A. Wołowicz, Z. Hubicki, Chem. Eng. J. 152 (2009) 72.
[57] J. Cai, Y. Huang, Y. Guo, Electrochim. Acta 99 (2013) 22.

[58] A.R. Miedema, Z. Metallkunde 69 (1978) 287.
[59] S. Demirel, M. Lucas, J. Wärnå, T. Salmi, D. Murzin, P. Claus, Top. Catal. 44 (2007) 299.
[60] B. Zhou, S. Hermans, G. Somorjai, Nanotechnology in Catalysis, Springer Science+Business Media New York, 2004.

**Tables**

Table 1 Actual metal content and particle size of the Pd-Bi/Dowex®1x4 catalysts

| | Loading [a] | | Pd size [b] |
|---|---|---|---|
| | Pd | Bi | (nm) |
| C3-1H | 2.9 | 1.1 | 5.5 |
| C3-1B | 2.9 | 1.1 | 3.4 |
| C3-03B | 2.9 | 0.3 | 3.9 |
| C3-05B | 2.8 | 0.6 | 3.8 |
| C3-3B | 2.8 | 3.1 | 3.4 |
| C3-45B | 2.7 | 4.6 | 2.9 |
| C2-06B | 2.1 | 0.6 | 2.6 |
| C1-03B | 1.0 | 0.3 | 2.8 |

[a] Weight % of Pd and Bi detected by AES-ICP and AAS-F methods, respectively
[b] Average diameter of Pd particles determined from XRD analysis for the half-with of the main Pd peaks corresponding to the (1 1 1) reflection

Table 2 Influence of reduction methods and amount of metals loaded on catalytic performance of Pd-Bi-NPs stabilized within Dowex 1x4 [a]

| | $r_{init}$ [b] | $t_{50}$ [c] | $X_{GLY}$ [d] | Selectivity [e] (%) | | | | | Y [f] (%) |
|---|---|---|---|---|---|---|---|---|---|
| | | (min) | (%) | GLYA | TARA | GLYCA | FORMA | OXA | GLYA+TARA |
| C3-1H | 51 | 75 | 93 | 59 | 14 | 6 | 7 | 2.2 | 59 |
| C3-1B | 78 | 50 | 95 | 68 | 15 | 4 | 10 | 1.1 | 63 |
| C2-06B | 42 | 100 | 68 | 59 | 14 | 10 | 4 | 1.1 | 48 |
| C1-03B | 25 | 260 | 47 | 51 | 14 | 12 | 2 | 1.1 | 29 |

[a] – Reaction conditions: as seen in Fig. 7, [b] – Initial reaction rate (mmol $L^{1-}$ $h^{1-}$) determined after 0.5 h of reaction, [c] – reaction time to achieve 50 % glycerol conversion, [d] – conversion of glycerol after 3 h of reaction, [e] – selectivity to glyceric acid (GLYA), tartronic acid (TARA), glycolic acid (GLYCA), formic acid (FORMA) and oxalic acid (OXA), respectively at 50 % of glycerol conversion, [f] – yield of Σ(glyceric acid and tartronic acid) after 3 h of reaction.